

Multiplexed ion beam imaging (MIBI) of human breast tumors

Michael Angelo, Sean C. Bendall, Rachel Finck, Matthew B. Hale, Chuck Hitzman, Alexander D. Borowsky, Richard M. Levenson, John B. Lowe, Scot D. Liu, Shuchun Zhao, Yasodha Natkunam, Garry P. Nolan

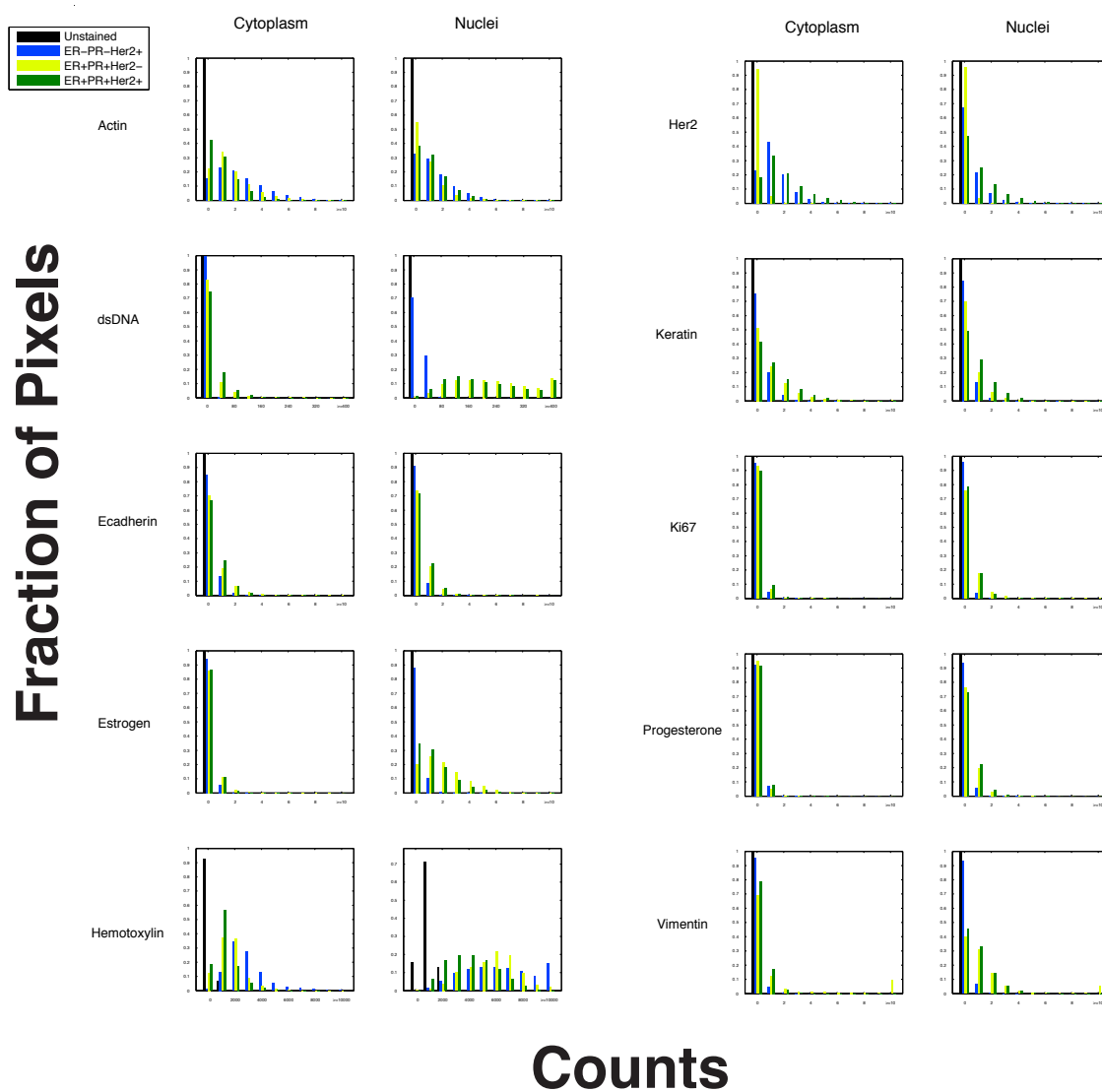


Figure S1. Histogram analysis of pixel intensities from MIBI breast tumor analysis. In tumor samples stained with metal-labeled antibodies, the distribution of pixel intensities for each marker varies according to tumor positivity and subcellular localization. In contrast, nearly all pixel values in a negative control sample are zero for all markers. The mean pixel intensity for all lanthanide channels within cytoplasmic and nuclear ROIs ranged between 0.0003–0.0025 and 0.00030–0.0032, respectively.

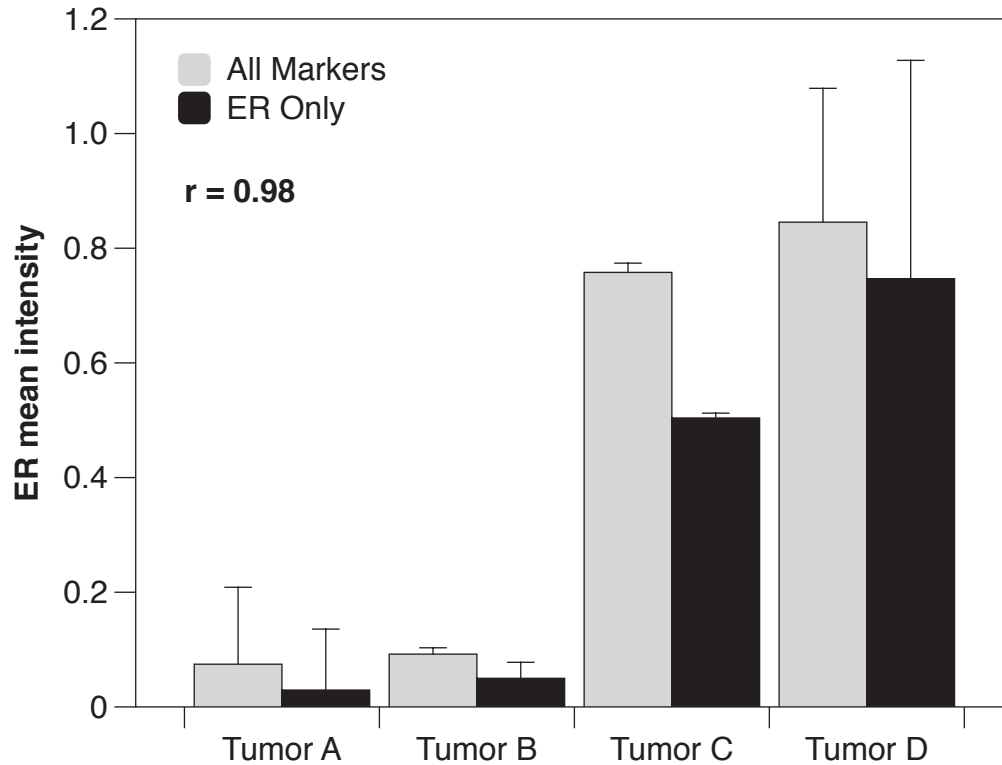


Figure S2. Comparison of ER intensity in serial sections stained with nine antibodies or ER only. ER staining intensity of breast tumors stained with hematoxylin and all nine antibodies (All Markers) used in the paper were compared with serial sections stained with hematoxylin and ER only (Fig. S4). This demonstrated very close correlation between the two methods. Linear regression of All Markers vs. ER only yielded Pearson Correlation of 0.98 ($P = 0.02$) and slope of $0.83 \pm 0.17SD$. The modest decrease in ER signal intensity observed with ER only samples can likely be explained by the inclusion of some non-tumor nuclei, since these samples did not include a keratin channel for masking tumor-free regions, as well as variations between serial sections.

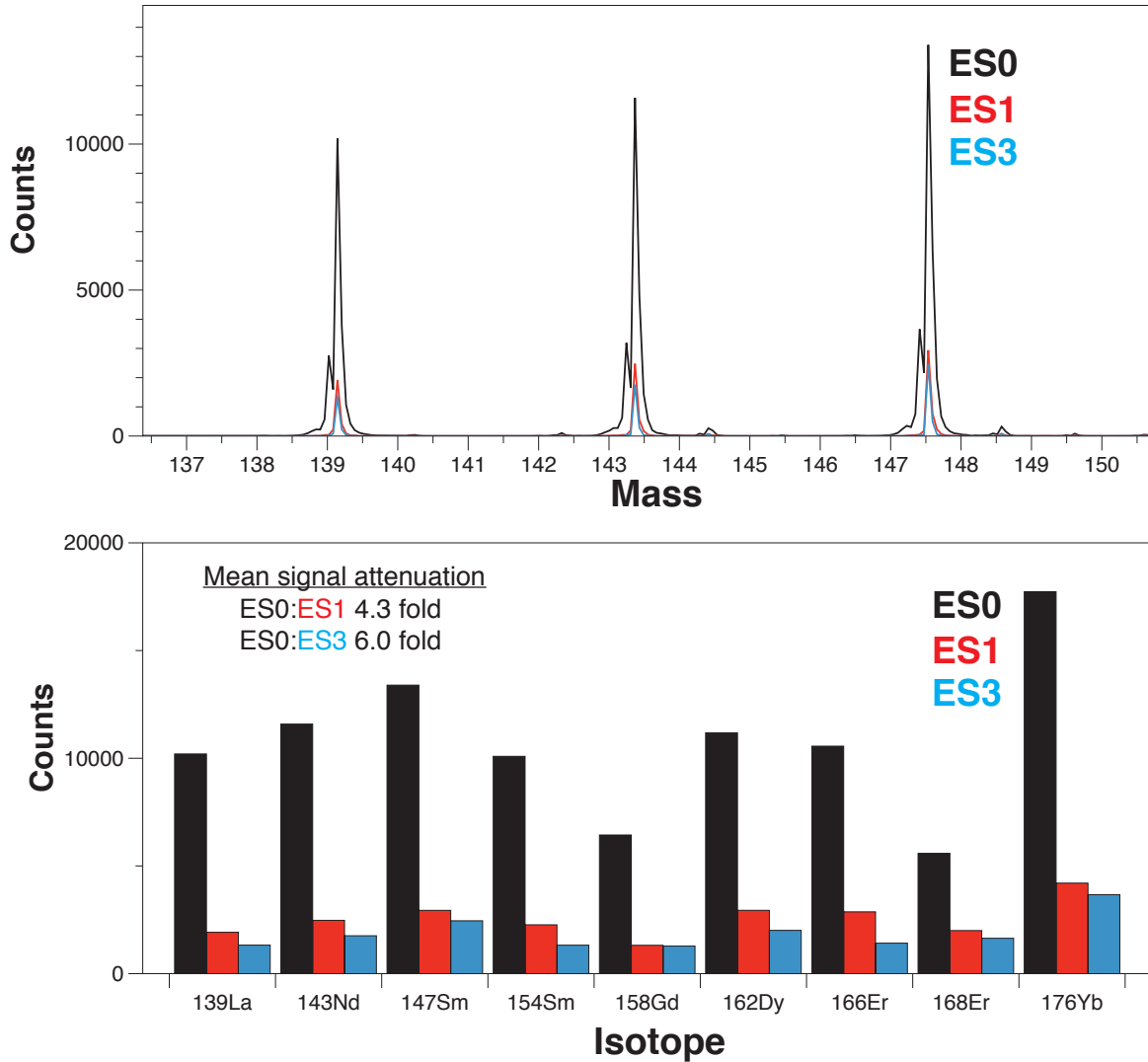


Figure S3. The effect of entrance slit width on mass resolution and signal intensity. Although mass resolution is improved when using smaller entrance slit values, ion transmission is appreciably attenuated. Because only unit resolution is needed to resolve the enriched isotope masses of interest in MIBI analysis, an entrance slit is not required.

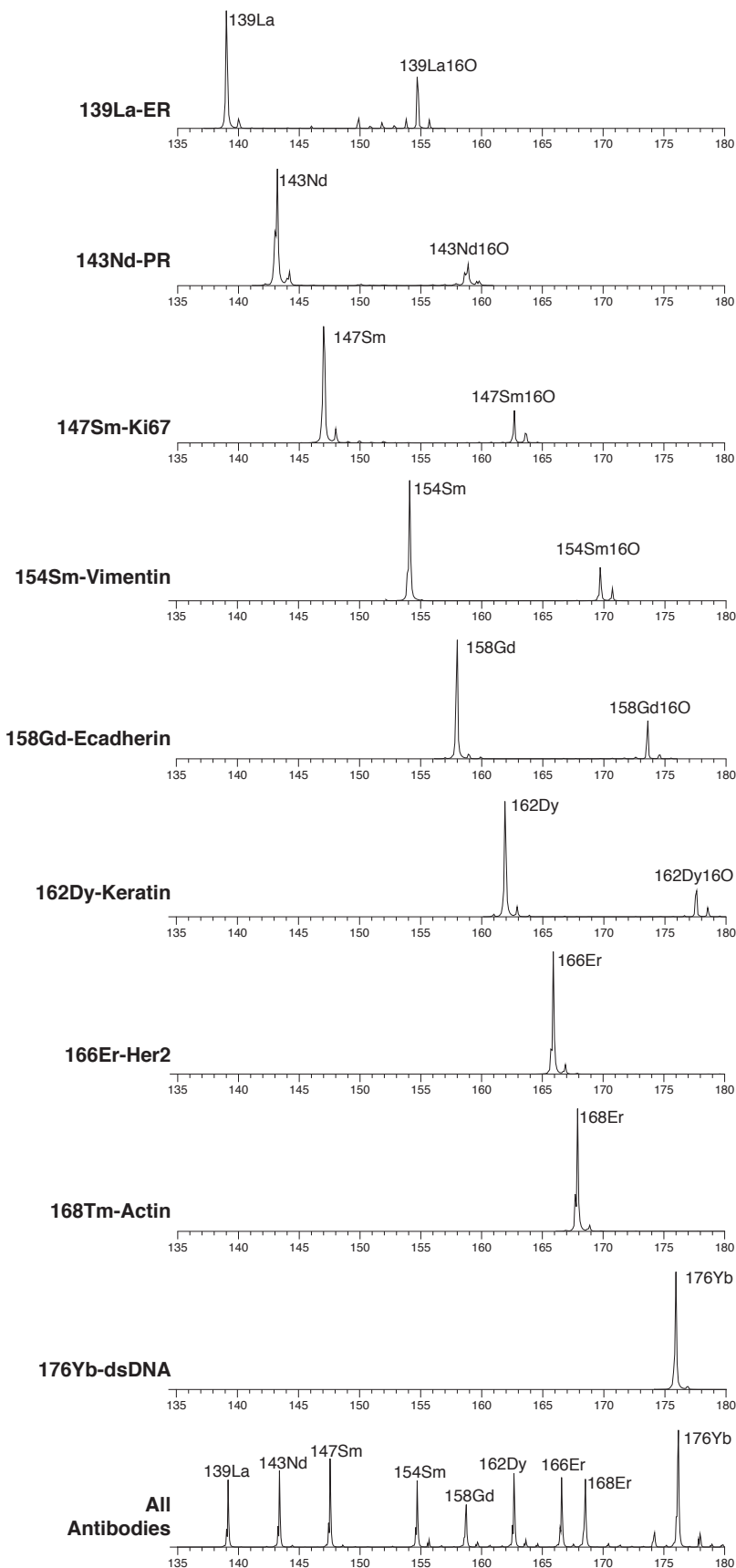


Figure S4. Full NanoSIMS spectral scans of metal conjugated antibodies. Mass spectral scans attained using a single detector while varying the B-field are shown for metal-tagged antibody standards for each isotope in isolation and in a mixture. Droplets of antibody master mix were deposited on a piece of clean silicon, allowed to air dry, and were then measured. Primary elemental peaks are non-overlapping and are unaffected by metal oxide adducts.

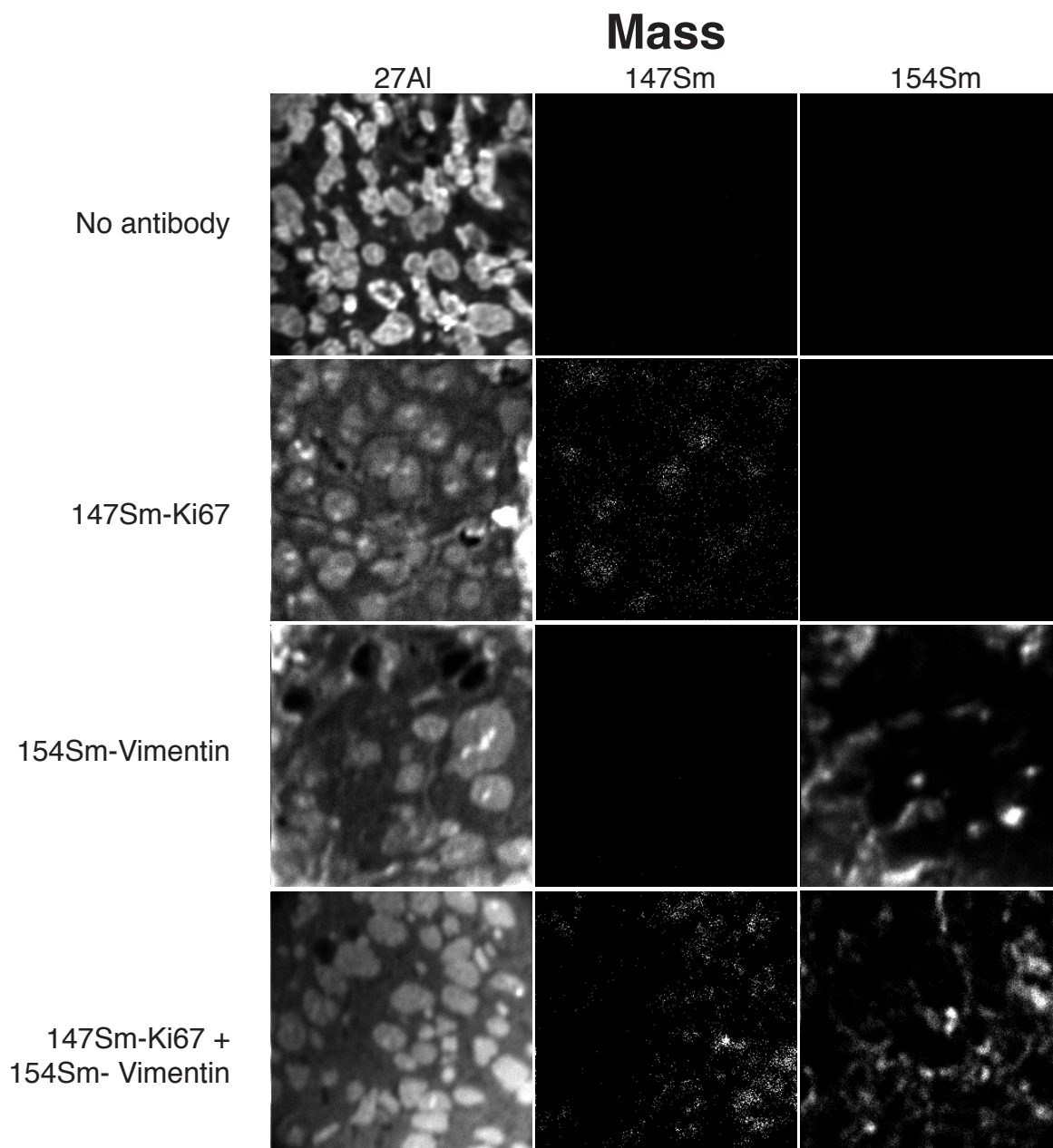


Figure S5. Assessment of channel crosstalk due to contaminating isotopic species using sections stained with single or multiple antibodies. Four serial sections were stained using (a) No antibodies, (b) 147Sm-Ki67, (c) 154Sm-Vimentin, or (d) 147Sm-Ki67 and 154Sm-Vimentin. Background signal in the control section and channel crosstalk between 147Sm and 154Sm in tissue sections stained with a single antibody were virtually non-existent. These results support the findings outlined in Fig. S1, S2, and S3, further demonstrating the absence of false positive signal due to contaminating isobaric or isotopic species.

mass →	139	140	141	142	143	144	145	146	147	148	149	150	151	152	153	154	155	156	157	158	159	160	161	162	163	164	165	166	167	168	169	170	171	172	173	174	175	176		
tag ↓																																								
La139	100																																							
Nd143				.85	96.4	2.22	.23	.26																																
Sm147									96.5	2.18	.52	.21		.41		.21																								
Sm154											.2			.91		98.9																								
Gd158																	.2	1.02	98.0		.82																			
Dy162																						1.39	94.1	3.67	.88															
Er166																											98.2	1.36	.46											
Er168																											.3	.71	98.5		.49									
Yb176																																				.27		99.7		

Table S1: ICP-MS analysis of enriched elemental isotopes for antibody labeling. The purity of enriched metal reagents used in this study are shown. Grey boxes denote the relative abundance of the intended elemental isotope (i.e. 139 for La139, 143 for Nd143). White boxes denote the relative abundance of residual contaminating isotopic or isobaric species.

PBMC Primary Antibodies					
<i>Antigen</i>	<i>Vendor</i>	<i>Clone</i>	<i>Mass</i>	<i>Staining Concentration</i>	<i>Element</i>
CD45	Biologend	HI30	115	2 $\mu\text{g mL}^{-1}$	In
CD19	DVS Sciences	HIB19	142	1:100	Nd
CD4	DVS Sciences	RPA-T4	145	1:100	Nd
CD14	DVS Sciences	M5E2	160	1:100	Gd
CD8	Biolognd	RPA-T8	165	2 $\mu\text{g mL}^{-1}$	Ho
CD3	DVS Sciences	UCHT1	170	1:100	Er
HLA-DR	DVS Sciences	L243	174	1:100	Yb
Breast Tumor Primary Antibodies					
ER alpha	Labvision	1D5	139	10 $\mu\text{g mL}^{-1}$	La
PR	cellsignal	D8Q2J	145	10 $\mu\text{g mL}^{-1}$	Nd
Ki67	Labvision	Polyclonal	150	10 $\mu\text{g mL}^{-1}$	Nd
Vimentin	Cellsignal	D21H3	154	10 $\mu\text{g mL}^{-1}$	Sm
E-cadherin	Cellsignal	24E10	158	10 $\mu\text{g mL}^{-1}$	Gd
Pan-keratin	Cellsignal	C11	162	10 $\mu\text{g mL}^{-1}$	Dy
Her2	Cellsignal	D8F12	166	10 $\mu\text{g mL}^{-1}$	Er
Pan-actin	Cellsignal	D18C11	168	10 $\mu\text{g mL}^{-1}$	Er
dsDNA	Abcam	HYB331-01	176	10 $\mu\text{g mL}^{-1}$	Yb

Table S2 – Antibody and metal reagents. The vendor, clone, mass tag, and staining concentration used for PBMC and tissue section analysis are shown.